PROCEEDINGS OF SCIENCE

High-efficiency, high-resolution SPECT techniques for cardiac imaging

Roberto Accorsi[1]
The Children's Hospital of Philadelphia
34th and Civic Center Blvd., Philadelphia PA 19104, USA.
E-mail: accorsi@email.chop.edu

Current standard clinical SPECT techniques provide a resolution of at best 1 cm and sensitivity in the order of 10^{-4}. Performance is largely determined by the collimator. Basic geometry couples resolution and sensitivity; the problem of high-resolution imaging is a formidable one because, to image at constant Signal-to-Noise, resolution improvements must be supported by simultaneous sensitivity improvements that scale with the fourth power of resolution. However, current standard systems are designed to also accommodate whole body studies and, thus, routinely provide large-area detectors. Single-organ imaging does not need the same field of view, which, then, can be better utilized with collimation schemes that magnify or cast more copies (i.e. acquire several views) simultaneously on the detector. As demonstrated by the recent experience of small animal imaging, these collimation techniques can be readily coupled to existing detectors to offer better performance than standard parallel-hole collimation. Similar approaches have been explored for a number of years for cardiac imaging. The same ideas also apply to other single-organ studies (e.g. brain and breast) as well as to pediatric imaging.

Frontiers in Imaging Science: High Performance Nuclear Medicine
Imagers for Vascular Disease Imaging (Brain and Heart)
Istituto Superiore di Sanita', Rome, Italy
13-14 November, 2006

[1] Speaker

PoS(FISBH2006)001

1. Introduction

The development of different collimation techniques for Single Photon Emission Computed Tomography (SPECT) has been an active area of research since the introduction of the simplest collimation devices for an Anger camera, i.e. the pinhole and the parallel-hole collimator. Converging collimation was first proposed in 1968 for thyroid imaging [1]; interest for pediatric, renal and cardiac studies followed soon [2]-[6]. Over the years various types of collimators have been proposed, such as slant-hole collimators [7] or the rotating slat collimator [8]-[10]; some were proposed specifically for cardiac imaging, e.g. the seven-pinhole collimator [11], [12]. More recently, small animal imaging posed the problem of high-resolution high-sensitivity imaging on an unprecedented scale. A number of systems based on custom detectors has been described [13]-[15], but applications to small-animal brain [16], bone [17], [18] and cardiac [17], [19] studies have clearly shown that SPECT can and does achieve sub-millimeter resolution on dedicated scanners as well as on adaptations of a clinical scanner calibrated accurately [20], [21].

Several factors characterize the performance of a SPECT system; the most obvious are Field of View (FoV), resolution, sensitivity, dose, imaging time and the presence or lack of artifacts in the reconstructed image. For a given cost, it is very hard to realize systems that can improve on all these factors simultaneously; while detector technology advances, optimizing the use of available technology is mostly related to taking advantage of the opportunities offered by the problem at hand to respond to its challenges. In the following, a more detailed discussion is presented of how small animal imaging gives an excellent example of such an optimization; the concept also applies to single-organ human imaging. Brief considerations on multiplexing systems and detector development are also offered.

2. Preliminary considerations

A rich choice of collimation options is available to SPECT system designers: next to parallel-, fan- and pinhole collimators, which are used in clinical practice, cone-beam, multiple pinhole, slant-hole, slat and slit-slat collimators have been under investigation for several years. Further, each collimator is available in versions offering flexible imaging conditions, e.g. high resolution vs. high sensitivity, or image very low (e.g. ^{125}I, 27-35 keV), low (^{99m}Tc, 140 keV), medium (^{67}Ga, 300 keV) or high energy (^{131}I, 365 keV, and PET isotopes, 511 keV) photons. The relationships between the resolution, sensitivity and FoV of these collimators have been explored analytically and experimentally: each collimator presents different trade-offs, the details of which are presented in the following section for the case of parallel-hole, converging and diverging collimators as well as for the pinhole collimator.

2.1 Pinhole collimation

In pinhole collimation all photons must reach the detector passing through a small (a few millimeters in diameter) aperture. Pinhole collimation is the case for which the calculation of resolution, sensitivity and FoV is easiest. Sensitivity is defined as the fraction of emitted

photons that contribute to the image. In the case of the pinhole, it is immediately related to the solid angle subtended by the pinhole's opening. For a round pinhole sensitivity is:

$$g = \frac{\frac{\pi}{4} w^2}{4\pi r^2} \sin\theta = \frac{w^2}{16 h^2} \sin^3\theta \tag{1}$$

where w is the diameter of the pinhole, r the distance from the pinhole to the point at which sensitivity is evaluated, h the distance from the same point to the plane of the pinhole and θ is the incidence angle that the photon path connecting the source to the center of the pinhole forms with the plane of the pinhole. Typical parameters can be used in (1) to show that typical pinhole collimators pass only one photon in 10,000. SPECT is particularly insensitive, and this limit is imposed by the collimator. It is for this reason that optimal performance entails optimal collimation design. Resolution is defined as the minimum distance that can separate two point sources before they become indistinguishable in the image due to collimator and detector blurring. For a pinhole collimator, resolution is given by the expression

$$\lambda_{sys} = \sqrt{\left(w \frac{h+f}{f} \right)^2 + \left(\frac{h}{f} R_i \right)^2} \tag{2}$$

where R_i is the intrinsic point spread function of the detector and f the focal length, i.e. the distance from the plane of the pinhole to the plane of the detector. From the definition, a small numerical value of resolution is desirable and is referred to as "high resolution" in common speech. The ratio f/h represents the ratio of the size of the projection of the object on the detector to the size of the object itself and is the magnification m of the imager. It also enters the expression for the field of view:

$$FoV = \frac{h}{f} D \tag{3}$$

where D is the size of the detector.

These expressions show some very basic properties of pinhole collimation: sensitivity depends strongly on w, but the use of large pinholes to increase sensitivity results in compromised resolution; an alternative is to image closer to the object (shorter h), but this implies a cost in FoV. It is for this reason that pinholes are used clinically in cases in which a relatively small FoV is sufficient, as in thyroid and testicular imaging in a general population or static renal imaging in infants.

In a broad sense this discussion is representative of all collimation choices: for a given detector, the improvement of one parameter implies a loss in some other parameter. Optimal use is achieved when the improvement is well worth the cost, which can very well be irrelevant (e.g. a reduced FoV when only a limited FoV is needed).

2.2 Parallel-hole, converging and diverging collimators

The sensitivity of collimators based on channels is given by the expression:

$$g = K \frac{d^4}{a_e^2 (d+t)^2} \left(\frac{f}{f-b} \right)^n \tag{4}$$

where d is the width of each channel, $a_e = a - 2/\mu$ its effective length, a its physical length, μ the linear attenuation coefficient in the material of the septa at the energy of the photons, t the thickness of the septa, and f and b are, respectively, the focal length of the collimator and the distance from the point at which sensitivity is being calculated measured from the patient side of the collimator; finally, $n = 0$ for parallel-beam, $n = 1$ for fan-beam and $n = 2$ for cone-beam collimators and K is a factor that accounts for different hole shapes (e.g. square vs. round or hexagonal). The case of the parallel beam is also found for $f \to \infty$. The expressions for diverging collimators simply use a negative value for f.

Resolution is given by the expression

$$\lambda_{sys} = \sqrt{\left(d\frac{a+b}{a}\right)^2 + \left(\frac{R_i}{f+a}(f-b)\right)^2} \tag{5}$$

Magnification is given by $m = |(f+a)/(f-b)|$. The field of view is

$$FoV = \frac{D}{m}. \tag{6}$$

These equations show several aspects, such as the well-known fact that the sensitivity of a parallel-hole collimator does not depend on the distance from the collimator. For this discussion it is more important to note that both sensitivity and resolution are connected to the ratio d/a: as for the hole width in the case of a pinhole, if d/a is decreased to improve resolution, at the same time sensitivity must decrease. In a converging collimator, sensitivity and resolution are very close to those of a parallel-hole collimator when the source is in contact with the collimator; however, unlike for the parallel-hole collimator, as b increases, sensitivity improves until the focal locus is reached. Again, the price is paid in terms of a decreasing FoV.

2.3 Slit-slat collimation

An interesting mix of the properties of pinhole and cone-beam collimation is found in slit-slat collimation, a technique first used in the early '80s [22]-[24] that has recently received renewed attention [25]-[27]. In this technique, slats are used axially to separate different planes of the object: axially slit-slat collimation works as parallel- or fan-beam collimation. The slit runs axially and is placed between the patient and the slats, to which it is perpendicular, providing collimation within each transaxial plane just as a pinhole. Accordingly, resolution expressions are essentially the same as those for pinhole collimation in transverse planes and the same as those for parallel- (or fan-) beam collimation along the axial direction. The sensitivity dependence is more complex and has experimentally been shown to be [27]:

$$g = \frac{wd^2}{4\pi ah(d+t)} \tag{7}$$

where w is the width of the slit, d the open space between two slats, t the thickness of the slats, a their height and h the distance from the point at which sensitivity is measured to the plane of the slit. A summary of resolution and sensitivity equations for all collimators seen so far is provided in Figure 1.

The sensitivity of a slit-slat collimator, thus, is maximum near the slit, where resolution is best.

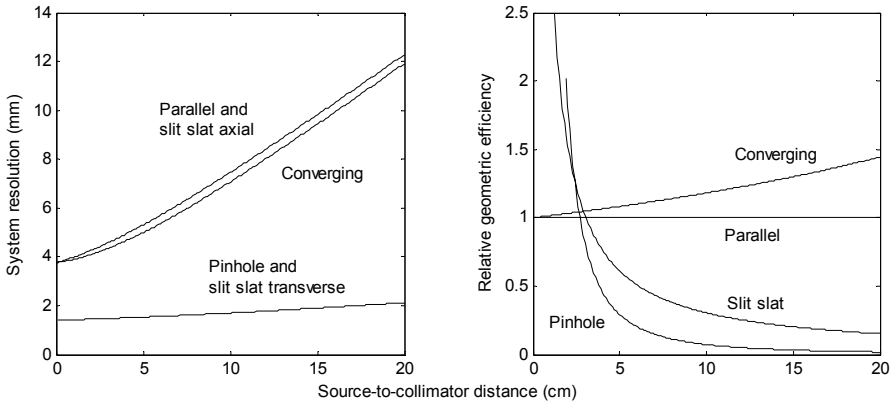

Figure 1: Resolution and sensitivity of different collimators for typical parameters. Pinhole diameter and septal or slit width 1.4 mm, septal thickness 0.18 mm, septal height 27 mm, fan-beam focal distance 650 mm. Intrinsic resolution of the detector: 3.5 mm FWHM. If the slit-slat collimator had been designed to have the same transverse resolution as the fan-beam collimator, its sensitivity would be higher, which would show a larger maximum RoR for which slit-slat collimation has an advantage over fan-beam collimation.

2.4 Multiplexing systems

The use of more than one pinhole improves sensitivity in a very obvious way, but it does have consequences. Since each pinhole casts a projection of the object onto the detector, a choice must be made between limiting magnification to prevent overlap of the copies or preserving relatively high magnification (and resolution) but allow overlap (often referred to as multiplexing). In the former case, a price in resolution and a limit in the number of pinholes must be paid; in the latter, the trade-off is more complex.

Optimal utilization of a pinhole entails placing the pinhole as close to the object as the FoV allows, i.e. the FoV is magnified to cover all of the detector's area. In these conditions, adding more pinholes certainly increases the sensitivity and, if the pinholes added have the same size as the original, resolution and FoV are preserved. However, overlap in the data alters the simple relationship between sensitivity and the Signal-to-Noise Ratio (SNR) of non-multiplexing systems, for which, according to Poisson statistics, the SNR is the square root of sensitivity. In systems with extreme overlap, in which hundreds of pinholes are used, this is still true for a point source, because there can still be no overlap; but the relationship between SNR and sensitivity changes as the distribution of activity over the FoV changes. For a point source, the increase in SNR equals the square root of the number of pinholes; as increasingly extended sources are used, the advantage is reduced from this theoretical limit; in some systems it will actually turn into a loss, depending on activity distributions ([28] and references therein). Furthermore, Poisson properties may be lost. In a non-multiplexed projection the mean and the variance image are the same because for Poisson counts mean and variance are the same. In coded aperture imaging, which uses multiplexing extensively, SNR is concentrated at bright spots in the image at the expense of SNR in photopenic regions. An evident example is again that of a point source: a point source becomes visible much sooner on a coded aperture image than on a pinhole image; but background will also show a much higher fluctuation on the coded

aperture image. Most relevant cases involve extended activity distributions. For example, breast imaging, in which the task is to identify hot uptake spots, may still seem a good application for coded aperture imaging; however this is not so because the vast majority of the activity is in fact normal uptake in healthy tissue, which creates a vast background from which the hot spots are only minor deviations in terms of total activity. It is for this reason that what seems to be a hot spot imaging task is, in the mathematical sense of coded aperture SNR theory, a case of a diffuse object.

2.5 Sampling completeness artifacts

It was already discussed how moving a pinhole closer to the object improves sensitivity and resolution at the cost of FoV; another parameter, sampling completeness, should also be considered.

The question of how much data are necessary for the artifact-free reconstruction of a volume has been investigated for various geometries. In a parallel-beam geometry a necessary and sufficient condition was first given by Orlov [33]. The condition is expressed in terms of the sphere of directions: each direction along which a projection of the object is formed on the detector determines a point on this sphere and the set of the directions of all projections determines a line, the vantage points line. Complete sampling is obtained, and thus artifact-free reconstruction is possible, if on the sphere of directions no great circle can be found that does not intersect the vantage points line.

In parallel-beam geometry the vantage point curve does not change if different points in the scan volume are chosen. But this is not the case in cone-beam geometry ([34]), which includes the case of pinhole collimation and is similar to fan-beam collimation. In cone-beam geometry sampling completeness is a local concept and should be evaluated at all points in the field of view. For example, consider the case of a pinhole describing a circular orbit and a point in the object in the plane of the orbit. The vantage points line is a great circle, so that it is impossible to trace on Orlov's sphere a great circle that does not intersect the vantage points line. If a point outside the plane of the orbit is considered, the vantage point line is not a great circle and at least the great circle in the plane parallel to the plane of the vantage point line will not intersect the vantage point line: points outside the plane of the orbit are not completely sampled. It has been suggested that the area spanned by great circles that do not intersect the vantage points line is related to the degree of completeness [35]; more specifically, the smaller the area, the closer the data will be to completeness.

Consider again the point outside the plane of the orbit: as the pinhole is brought closer to the object to improve sensitivity and resolution, the vantage points line moves away from the great circle parallel to the plane of the orbit, showing that data are less and less complete. This results in increased axial blurring of reconstructed images [36]. It is for this reason that orbits other than circular have been proposed [37] and investigated [38].

3. Applications

The previous section illustrated how the basic principles of collimator design are so strictly related that improving some is typically obtained at a cost in some others. Regardless of

detector, dose or time are proportional to the fourth power of resolution at constant SNR; for this basic fact, "it is extraordinarily difficult to improve resolution in nuclear imaging" [29]. In fact, an improvement by a factor of two in resolution would need a concurrent improvement by a factor of 16 in sensitivity to preserve SNR. Nevertheless opportunities are still present for improved imaging.

3.1 Imaging distance

The most obvious approach to improve resolution is reducing the distance from the object whenever possible. The analysis of Section 2 shows that all collimators offer best resolution near the collimator. For this reason high-resolution designs strive to provide convenient access to the target organ. A simple, but good, example is the improvement over circular orbits offered by body contour orbits, which in posterior and anterior views remain closer to the patient than allowed by circular orbits. Parallel, slant–hole collimators can acquire oblique views of the heart with the detector positioned for an anterior view (with a regular parallel-hole collimator), i.e. at a lower distance than the right anterior oblique view otherwise needed. In breast imaging, detectors have been designed to minimize the inactive area on one of their sides, which can then be placed directly against the chest wall, with the breast resting on the collimator.

Short distances also increase sensitivity in pinhole and slit-slat collimation; the opposite is true for converging collimation.

3.2 Fan- and cone- beam collimation

A second approach relies on the large FoV of modern gamma cameras, which are already widely used in current clinical practice. Early gamma cameras were sufficiently large for single organ studies, but whole body studies required diverging collimators to avoid lengthy scanning of the patient over multiple bed positions. At about 40 cm × 50 cm (e.g. 38.1 cm × 50.8 cm. Epic HP detector. Philips Medical Systems, Andover, MA), the FoV of a current camera is significantly larger than needed in single-organ studies.

For single-organ imaging, i.e. cardiac, breast and brain imaging, thus, better uses of the FoV are possible than provided by a parallel-hole collimator. For example, conservative adult brain dimensions are 21 cm (sagittal) × 17.6 cm × 17.6 cm [30]. Using parallel-beam collimation would leave a considerable part of the detector unused.

Better detector utilization can be achieved with fan-beam collimation, which can be designed to project the brain on the whole transaxial extent of the detector. Performance can be further improved if it is possible to position the detector as close as possible to the head, i.e. using an orbit that clears the patient's shoulders.

Maximum detector utilization can also be achieved in the axial direction with cone beam collimation, but use of a circular orbit does not provide a dataset that can be reconstructed without artifacts in 3D (i.e. the dataset is incomplete). Different schemes have been proposed to overcome this limitation, such as using a parallel- [31] or fan- [30] beam collimator on one of the heads of a multiple-head system. Further, the focal point of the cone beam collimator can be shifted caudally to allow the detector to clear the shoulders of the patient. When the shift equals half of the axial extent of the detector, a half-cone beam collimator is obtained [31].

A particularly interesting application of the technique for a very specialized application involves using an ultra-short focal length (~20 cm) collimator [30]. This variation is based on the fact that the sensitivity of a converging collimator is maximum at its focus. If the focus is placed by design near the center of the brain, structures relevant in Parkinson and Alzheimer disease can be imaged with high sensitivity and a slight improvement in resolution with respect to longer focal length collimators (in the limiting case parallel-beam collimators). The advantage is restricted over the small area of interest, but an SNR advantage of about three (i.e. a factor of nine in time or dose) can be obtained (Figure 2).

For their properties, fan-beam collimators have also been used for cardiac imaging.

3.3 Slit-slat collimation

The resolution and sensitivity formulas for slit-slat collimation indicate that, for a given resolution, slit-slat collimators provide a compromise between pinhole and fan-beam collimation. In fact, sensitivity decreases with distance with a $1/h^2$ law in pinhole collimation, but only as $1/h$ in slit-slat collimation (Figure 1); therefore, for the same resolution, a radius must exist for which slit-slat collimators provide higher sensitivity than a pinhole. For even larger distances, however, fan-beam collimators, whose sensitivity increases with distance up to the focal length, will eventually show best sensitivity. It is for this reason that slit-slat collimation is expected to offer best performance when intermediate Radii of Rotation (RoRs) are used. The data of [27] suggest that 15 cm can be a reasonable estimate for the RoR upper bound, i.e. the value after which slit-slat collimators no longer offer an advantage. If cardiac imaging can be accomplished with shorter RoRs, slit-slat collimation is expected to be a competitive option. Indeed dedicated cardiac scanners based on slit-slat collimation have recently become commercially available [32].

Figure 2 also shows that a slit-slat collimator with converging slats provides even better performance than short focal length collimators in cortical regions (spheres 3 and 5) and

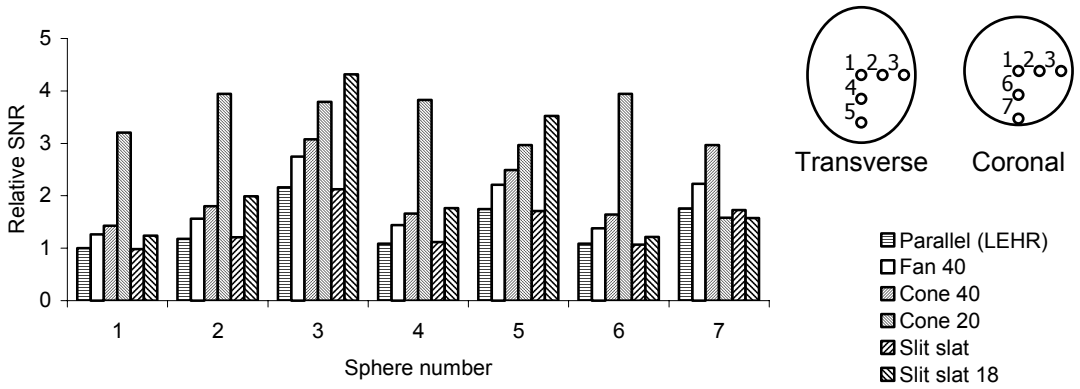

Figure 2: SNR of different collimators compared to the SNR achieved with a parallel-hole collimator pair for the sphere at the center of the brain (sphere 1). All non-parallel-hole collimators are assumed paired to a fan-beam collimator with focal length 40 cm to ensure data completeness. 'Cone 20' and 'cone 40' indicate a focal length of 20 and 40 cm, respectively. 'Slit slat 18' indicates slats converging with focal length 18 cm. All data produced (for slit slat collimation) or reproduced with the methods of [30].

performance comparable to a parallel-beam collimator otherwise. This finding is consistent with the observation that resolution and sensitivity are both best near the slit, whereas for a converging collimator sensitivity is best at the focal point, which is far from the collimator.

3.4 Small-animal imaging

Small animal imaging is the best example of a case in which a very small fraction of the FoV is necessary to cover the object. The reduced demand for FoV gives the opportunity to achieve high resolution at relatively constant sensitivity by using magnification and small diameter pinholes. The routine availability of large-FoV detectors on current clinical scanners opens the very same opportunity to single-organ imaging, albeit on a different scale.

3.5 Implications of geometric considerations on new detector development

The interest in the development of new detectors can be based on a number of factors, such as detection efficiency and energy resolution. A common motivation is also improved spatial resolution. For a given detector size, improved intrinsic resolution does lead to improved system resolution; however, it is important to realize that magnification couples resolution and FoV. For example, from (2) and (3) one gets:

$$\lambda_{sys} = \sqrt{\left(d\,\frac{h+f}{f} \right)^2 + \left(FoV\,\frac{R_i}{D} \right)^2} \tag{8}$$

which shows that, for a given FoV, the intrinsic resolution of the detector R_i affects system resolution only through its ratio to the size of the detector. For pixelated detectors this ratio is the same as the number of pixels; for a large FoV Anger camera $D/R_i \sim 400$ mm / 3.5 mm > 100. If a small FoV is needed, a large-FoV detector with average intrinsic spatial resolution can be a competitive alternative to small-FoV detectors with good intrinsic spatial resolution. An advantage of continuous systems with Anger positioning is also the opportunity to locate events with arbitrary small sampling. Among other elements, the development of new detectors needs to take into account both the feasibility of a large FoV and its sampling.

4. Conclusions

The problem of high-resolution imaging in count-limited situations as in Nuclear Medicine, and especially in SPECT, is a very difficult one because an improvement by a factor of two in resolution entails an improvement by a factor of sixteen in sensitivity for imaging at constant SNR.

High resolution can be achieved by imaging as close as possible to the target; for this reason, collimators and cameras that provide ready access to the patients have been designed. Contemporary clinical systems make widely available large FoV cameras designed to accommodate whole body imaging. Single-organ imaging on these systems can be (and is routinely) accomplished with parallel-beam collimation, which, however, does not utilize the whole detector. This opens the opportunity to design magnifying optics or acquiring simultaneously several copies of the limited FoV needed. Although magnifying collimators have long been available, their use in clinical practice is still not widespread in spite of

improved performance, possibly because their use on systems with interchangeable collimators increases the complexity of the system. In the near future it is possible that cameras dedicated to a specific application (i.e. cardiac perfusion) will find a commercial environment favorable to their dissemination. On such systems, it is possible to mount non-interchangeable optics without sacrificing performance while keeping complexity to a minimum. Some of these systems are already commercially available.

References

[1] R.N. Beck, *Collimation of gamma rays*, in *Fundamental problems in scanning*, A. Gottschalk and R.N. Beck eds, Springfield, Ill, CC Thomas, 1968

[2] J.E. Dowdey, K.D. Graham, and F.J. Bonte, *Collimator magnification of scintillation camera images*, *J. Nucl. Med.* **12** (352) 1971

[3] S. Rudin, P.A. Bardfeld, and H. Hart, *Use of magnifying multihole collimators in the gamma-ray camera system*, *J. Nucl. Med.* **12** (831) 1971

[4] S. Rudin, K.L. Rider, and H.E. Hart. *A tomographic magnifying collimator system for the gamma camera*, *Radiology* **102** (371) 1972

[5] J.E. Dowdey and F.J. Bonte *Principles of scintillation camera image magnification with convergent collimators*, *Radiology* **104** (89) 1972

[6] R. A. Moyer, *A low-energy multihole converging collimator compared with a pinhole collimator*, *J. Nucl. Med.*, **15** (59) 1974

[7] W. Chang, S. L. Lin, and R. E. Henkin, *A new collimator for cardiac tomography: the quadrant slant-hole collimator*, *J. Nucl. Med.* **23** (830) 1982

[8] W. I. Keyes, *The fan-beam gamma camera*, *Phys. Med. Biol.*, **20** (489) 1975

[9] M. A. Lodge, D. M. Binnie, M. A. Flower, and S. Webb, *The experimental evaluation of a prototype rotating slat collimator for planar gamma camera imaging*, *Phys. Med. Biol.*, **40** (427) 1995

[10] G. L. Zeng and D. Gagnon*, Image reconstruction algorithm for a spect system with a convergent rotating slat collimator*, *IEEE Trans. Nucl. Sci.*, **51** (142) 2004

[11] R.A. Vogel, D. Kirch, M. LeFree, and P. Steele, *A new method of multiplanar emission tomography using a seven pinhole collimator and an Anger scintillation camera*, *J. Nucl. Med.* **19** (648) 1978

[12] T. Funk, D. L. Kirch, J. E. Koss, E. Botvinick, and B. H. Hasegawa, *A novel approach to multipinhole SPECT for myocardial perfusion imaging*, *J. Nucl. Med.* **47** (595) 2006

[13] D.P. McElroy, L.R. MacDonald, F.J. Beekman, Y. Wang, B.E. Patt, J.S. Iwanczyk, B.M.W. Tsui, and E.J. Hoffman, *Performance evaluation of A-SPECT: a high resolution desktop pinhole SPECT system for imaging small animals*, *IEEE Trans. Nucl. Sci.*, **49** (2139) 2002

[14] G.A. Kastis, L.R. Furenlid, D.W. Wilson, T.E. Peterson, H. B. Barber, and H.H. Barrett, *Compact CT/SPECT small-animal imaging system*, *IEEE Trans. Nucl. Sci.*, **51** (63) 2004

[15] A. G. Weisenberger, S. S. Gleason, J. Goddard, B. Kross, S. Majewski, S. R. Meikle, M. J. Paulus, M. Pomper, V. Popov, M. F. Smith, B. L. Welch, and R. Wojcik, *A restraint-free small animal SPECT imaging system with motion tracking*, *IEEE Trans. Nucl. Sci.*, **52** (638) 2005

[16] P. D. Acton, S.-R. Choi, K. Plössl, and H. F. Kung, *Quantification of dopamine transporters in the mouse brain using ultra-high resolution single-photon emission tomography*, *Eur. J. Nucl. Med.* **29** (691) 2002

[17] F. J. Beekman, F. van der Have, B. Vastenhouw, A. J.A. van der Linden, P. P. van Rijk, J. P. H. Burbach, and M. P. Smidt. *U-SPECT-I: a novel system for submillimeter-resolution tomography with radiolabeled molecules in mice*, *J. Nucl. Med.* **46** (1194) 2005

[18] B. Ostendorf, A. Scherer, A. Wirrwar, J. W. Hoppin, C. Lackas, N. U. Schramm, M. Cohnen, U. Mödder, W. B. van den Berg, H. W. Müller, M. Schneider, and L. A. B. Joosten, *High-resolution multipinhole single-photon-emission computed tomography in experimental and human arthritis*, *Arthritis & Rheumatism*, **54** (1096) 2006

[19] S. Vemulapalli, S. D. Metzler, G. Akabani, N. A. Petry, N. J. Niehaus, X. Liu, N. H. Patil, K. L. Greer, R. J. Jaszczak, R. E. Coleman, C. Dong, P. J. Goldschmidt-Clermont, and B. B. Chin, *Cell Therapy in Murine Atherosclerosis: In Vivo Imaging with High-Resolution Helical SPECT*, *Radiology*, **242** (198) 2007

[20] D. Bequé, J. Nuyts, G. Bormans, P. Suetens, and P. Dupont, *Characterization of pinhole SPECT acquisition geometry*, *IEEE Trans. Med. Imag.*, **22** (599) 2003

[21] S. D. Metzler and R. J. Jaszczak, *Simultaneous multi-head calibration for pinhole SPECT*, *IEEE Trans. Nucl. Sci.*, **53** (113) 2006

[22] W. L. Rogers et al., *SPRINT: A stationary detector single photon ring tomography for brain imaging, IEEE Trans. Med. Imaging*, **MI-1** (63) 1982

[23] W. L. Rogers et al., *Performance evaluation of SPRINT: a single photon ring tomograph for brain imaging, J. Nucl. Med.* **25** (1013) 1984

[24] W. L. Rogers et al., *SPRINT II: A second generation single photon ring tomograph," IEEE Trans. Med. Imaging* **7** (291) 1988

[25] S. Walrand, F. Jamar, M. de Jong, and S. Pauwels, *Evaluation of novel whole-body high-resolution rodent SPECT (linoview) based on direct acquisition of linogram projections*, *J. Nucl. Med.*, **46** (1872) 2005

[26] D. Brasse, I. Piqueras, and J.-L. Guyonnet, *Development of a high resolution SPECT system dedicated to small animal imaging, in Proc. Nuclear Science Symposium Conf. Record, Rome,* (3868) 2004

[27] S. D. Metzler, R. Accorsi, J. R. Novak, A. S. Ayan, and R. J. Jaszczak, *On-axis sensitivity and resolution of a slit-slat collimator, J. Nuc. Med.*, **47** (1884) 2006

[28] R. Accorsi, F. Gasparini, and R. C. Lanza, *Optimal coded aperture patterns for improved SNR in nuclear medicine imaging*, *Nuclear Instruments and Methods in Physics Research A*, **474** (273) 2001

[29] H. Barrett and W. Swindell, *Radiological Imaging*, Academic Press, San Diego 1981

[30] M.-A. Park, S.C. Moore, and M. Foley Kijewski, *Brain SPECT with short focal-length cone-beam collimation*, *Med. Phys.* **32** (2236) 2005

[31] C.D. Stone, M.F. Smith, K.L. Greer, and R.J. Jaszczak, *A combined half-cone beam and parallel hole collimation system for SPECT brain imaging*, *IEEE Transactions on Nuclear Science*, **45** (1219) 1998

[32] W. Chang, H. Liang, and J. Liu, *Design concepts and potential performance of MarC-SPECT - A high-performance cardiac SPECT system*, *J. Nucl. Med.*, **47** (190P) 2006

[33] S. S. Orlov, *Theory of three dimensional reconstruction, Sov. Phys. Crystallogr.*, **20** (312) 1975

[34] H. K. Tuy, *An inversion formula for cone-beam reconstruction, SIAM Journal on Applied Mathematics*, **43** (546) 1983

[35] S.D. Metzler, J.E. Bowsher and R.J. Jaszczak, *Geometrical similarities of the Orlov and Tuy sampling criteria and a numerical algorithm for assessing sampling completeness*, *IEEE Trans. Nucl. Sci,* **50** (1550) 2003

[36] S.D. Metzler, K.L. Greer, K. Bobkov and R.J. Jaszczak, *Helical pinhole SPECT for small animal imaging: a method for addressing sampling completeness, IEEE Trans. Nucl. Sci.,* **50**, (1575) 2003

[37] B. D. Smith, *Image reconstruction from cone-beam projections: Necessary and sufficient conditions and reconstruction methods, IEEE Trans. Med. Imag.,* **MI-4** (14) 1985

[38] C.N Archer, M.P. Tornai, J.E Bowsher, S.D. Metzler, B.C. Pieper, and R.J Jaszczak, *Implementation and initial characterization of acquisition orbits with a dedicated emission mammotomograph, IEEE Transactions on Nuclear Science*, **50** (413) 2003